Journal of Materials Chemistry A

ROYAL SOCIETY OF CHEMISTRY

PAPER

View Article Online
View Journal | View Issue

Check for updates

Cite this: J. Mater. Chem. A, 2025, 13, 4940

Photocatalytic performance of $Y_2Ti_2O_5S_2$ prepared *via* carbon disulfide sulfurization†

Lihua Lin, [ab] Qin Li, [bc] Yuzuki Kanazawa,[d] Kiyoshi Kanie,[d] Mamiko Nakabayashi,[e] Chen Gu, [b] Daling Lu,[b] Takashi Hisatomi, [bf] Tsuyoshi Takata[b] and Kazunari Domen *[bfg]

Received 17th November 2024
Accepted 5th January 2025

DOI: 10.1039/d4ta08167f

rsc.li/materials-a

$Y_2Ti_2O_5S_2$ (YTOS) has a narrow bandgap and exhibits excellent stability, and so it is a potential high-performance oxysulfide photocatalyst for solar-driven water splitting to produce green hydrogen. However, YTOS is typically synthesized in sealed quartz tubes, often in the presence of flux reagents, and such processes are difficult to scale up for practical applications. Alternatively, YTOS can be synthesized using a stream of gaseous H_2S as a sulfurizing reagent but the reaction requires a high temperature and the resulting material suffers from a high density of defects and impurities. The present work demonstrates the synthesis of YTOS using carbon disulfide (CS_2) as a sulfurizing reagent in the presence of a flux. Owing to the high activity of CS_2 and the enhanced mass transfer provided by the flux, YTOS could be formed from oxide precursors at a lower temperature than that employed when using H_2S. The photocatalytic H_2 evolution activity of the resulting YTOS was greater than that of YTOS synthesized using the conventional solid-state reaction or H_2S sulfurization methods and comparable to that of YTOS prepared by the flux-assisted method. CS_2 sulfurization represents a new approach for the synthesis of functional oxysulfide photocatalysts in a manner that may be suitable for mass production.

Open Access Article. Published on 13 January 2025. Downloaded on 12/31/2025 11:32:42 AM.
This article is licensed under a Creative Commons Attribution 3.0 Unported Licence.

Introduction

$Y_2Ti_2O_5S_2$ (YTOS) is a promising oxysulfide water splitting photocatalyst.[1–3] This material has a narrow bandgap that permits the absorption of sunlight up to a wavelength of 650 nm, with a maximum solar-to-hydrogen energy conversion efficiency of approximately 20% assuming an apparent quantum yield of unity up to the absorption edge.[4] YTOS also exhibits outstanding stability compared with sulfides, making it is well-suited for long-term operation. In 2019, one-step excitation overall water splitting was achieved using YTOS after various surface modifications.[5] However, the resulting performance was much lower than expected, likely due to the large particle size and high defect density in the specimen.[6,7] For this reason, much effort has been dedicated to the preparation of high-quality YTOS crystals having modified surface properties as a means of improving catalytic activity.[8,9]

To date, crystalline YTOS has been primarily synthesized using the solid-state reaction (SSR) technique. In this procedure, Y_2O_3, Y_2S_3 and TiO_2 acting as precursors are thoroughly mixed and then transferred into a quartz tube, which is then evacuated and sealed. The tube is subsequently heated to a specific temperature and held at that temperature for a long time span (typically longer than four days) to complete the reaction.[10–13] This long duration is required because of the low mass transfer rate associated with the SSR process. The resulting YTOS tends to exhibit large particle sizes ranging from several micrometers to tens of micrometers, and bulk defects are often found in the crystals. Consequently, a flux-assisted method has been devised to address these issues. The ionic molten salt flux serves as a polar solvent to promote the formation and growth of YTOS when the calcination temperature is higher than the melting point of the flux. Therefore, the mass transfer enhancement can be partially ascribed to the dissolution of solid reactants by the flux and solvation of ions through strong polarization, followed by rapid migration of reactant species by convection and diffusion in the molten flux. The chemical reactivity of precursors is also enhanced due to the increased ionic mobility and contact area of reactants in the presence of flux.[14–17] In prior work, $Sm_2Ti_2O_5S_2$ (STOS) having

[a]College of Environment and Safety Engineering, Fuzhou University, Fuzhou 350108, Fujian Province, P. R. China
[b]Research Initiative for Supra-Materials, Interdisciplinary Cluster for Cutting Edge Research, Shinshu University, Nagano 380-8553, Japan
[c]Key Laboratory of Catalysis and Energy Materials Chemistry of Ministry of Education, South-Central Minzu University, Wuhan 430074, China
[d]Institute of Multidisciplinary Research for Advanced Materials, Tohoku University, Hongo, Bunkyo-ku, Japan
[e]Institute for Engineering Innovation, The University of Tokyo, Hongo, Bunkyo-ku, Tokyo 113-8656, Japan
[f]Institute for Aqua Regeneration, Shinshu University, Nagano 380-8553, Japan
[g]Office of University Professors, The University of Tokyo, Tokyo 113-86556, Japan. E-mail: domen@chemsys.t.u-tokyo.ac.jp

† Electronic supplementary information (ESI) available. See DOI: https://doi.org/10.1039/d4ta08167f

This journal is © The Royal Society of Chemistry 2025

Open Access Article. Published on 13 January 2025. Downloaded on 12/31/2025 11:32:42 AM.
This article is licensed under a Creative Commons Attribution 3.0 Unported Licence.

smaller particle sizes and increased crystallinity was obtained by using CsCl as a flux together with a significantly shortened calcination time. An enhanced mass transfer rate was provided by the flux. Materials produced using the flux-assisted method have also exhibited improved performance compared with those synthesized with the SSR method.[18–20] Subsequent to the above work, YTOS was prepared by a flux-assisted method using $CaCl_2$, $MgCl_2$ or LiCl/$MgCl_2$ fluxes.[21–23] In such cases, the particle sizes were significantly decreased while the degree of crystallinity was enhanced. In general, the decreased particle size shortens the migration distance of charges to the surface.[24–26] Meanwhile, bulk defects which act as recombination centers for electrons and holes can be reduced with the enhanced crystallinity.[27–30] Hence, the as-prepared photocatalysts exhibited improved performance when applied to both the H_2 and O_2 evolution half-reactions. Even so, both the SSR and flux-assisted techniques require a closed environment such as a sealed quartz tube to prepare oxysulfide materials, to avoid the loss of sulfur from the precursor and the product during high temperature synthesis. This requirement is not well-suited for the large-scale production of oxysulfide photocatalysts.

To address this issue, a sulfurization method was developed as an alternative synthesis approach, based on the use of H_2S as a sulfidation reagent to generate STOS from $Sm_2Ti_2O_7$.[31,32] Owing to the high sulfurization activity of H_2S, this process greatly reduces the calcination time from several days to approximately 1 h and also allows the reaction temperature to be lowered from 1000 to 800 °C compared with the SSR method when synthesizing STOS. More importantly, the primary particle diameter range of the STOS is decreased from 2–4 to 0.1–0.5 μm. Similar results have been obtained for the preparation of YTOS by the H_2S sulfidation method, although a relatively high temperature of 1150 °C is required in this case.[33] One advantage of the sulfurization method is that the synthetic equipment can be easily scaled up to allow large amounts of oxysulfide photocatalysts to be produced in a practical manner. However, the resulting materials tend to exhibit decreased performance compared with those produced using the SSR method, likely due to the reduced crystallinity and increased defect density. These effects are partly a consequence of H_2 generated from the H_2S employed during sulfidation. As such, it is important to investigate other sulfurization reagents that allow the production of functional oxysulfides under mild conditions.

In the present work, carbon disulfide (CS_2), which has been widely used in the synthesis of functional materials,[34–36] was employed as a new sulfidation reagent to prepare the YTOS photocatalyst. The flux-assisted method was also introduced to promote the formation reaction because only intermediate phases or binary sulfides were formed in the absence of flux. Due to the enhanced mass transfer and greater sulfurization activity obtained from this process, YTOS could be synthesized from a mixture of Y_2S_3, Y_2O_3 and TiO_2 or a mixture of Y_2O_3 and TiO_2 acting as the starting materials within a span of just several hours. In particular, the YTOS crystals resulting from oxide precursors exhibited reduced particle sizes and improved crystallinity compared with YTOS obtained using the SSR method, which also showed enhanced performance when applied to the sacrificial H_2 evolution reaction after suitable modifications.

Experimental section

Material preparation

Various precursors were utilized during the sulfurization reaction trials, including a combination of the conventional precursors Y_2O_3 (99%, Iwatani Corporation), Y_2S_3 (99.9%, Kojundo Chemical Laboratory Co. Lit.) and TiO_2 (99.99%, Rare Metallic Co., Ltd., rutile phase) combined in a molar ratio of 1 : 2 : 6, a mixture of Y_2O_3 and TiO_2 with a molar ratio of 1 : 2 or simply $Y_2Ti_2O_7$. The materials generated from these precursors by flux-assisted sulfurization are herein referred to as YTOS-YOYS, YTOS-YO, and YTOS-YTO, respectively. The $Y_2Ti_2O_7$ precursor was prepared by mixing Y_2O_3 and TiO_2 in a 1 : 2 molar ratio followed by heating at 1000 °C for 6 h in air. After being allowed to cool naturally, the product was ground to obtain finely powdered $Y_2Ti_2O_7$. Unless otherwise noted, all the precursors were mixed with $CaCl_2$ at a proportion of 500 wt%, which served as the flux, in preparation for flux-assisted sulfurization. In each case, the precursors and flux were ground together in a glovebox under a flow of high-purity nitrogen for 30 min using an agate mortar, after which 3.0 g of this mixture (including the $CaCl_2$) was transferred into an alumina boat. This boat was subsequently placed in a horizontal tube furnace. In the case where the $CaCl_2$ flux was not included, 0.5 g of the starting mixture was instead transferred to the alumina boat. A quantity of liquid CS_2 (99 wt% purity, Wako) was maintained at 10 °C to obtain a stable evaporation rate and a 22 mL min^{-1} flow of N_2 was passed through the liquid reagent to produce a gaseous CS_2/N_2 mixture. In some trials, an additional 100 mL min^{-1} flow of N_2 gas was blended with the CS_2/N_2 gas mixture for dilution. The sample was heated at 10 °C min^{-1} to 500 °C and then at 5 °C min^{-1} to 800 °C after which the material was held at that temperature for 3 h. After natural cooling to 300 °C, the CS_2/N_2 gas mixture was shut off while a continuous flow of N_2 gas was maintained for an additional 4 h to remove residual CS_2. The sample was subsequently sonicated in distilled water and the flux was removed by capturing the product *via* filtration. The as-obtained powder was dried by heating under vacuum at 40 °C for 4 h (Fig. S1a†). Finally, the product was heated at 200 °C in air for 1 h to remove residual sulfur on the surface of the material and again dispersed in distilled water by sonication followed by filtration and drying under vacuum for 4 h (Fig. S1b†). Unless noted otherwise, the CS_2/N_2 and N_2 flow rates during these syntheses were 22 and 100 mL min^{-1}, respectively, the precursor-to-flux ratio was 1 : 5 and the duration was 3 h. A post-treatment was applied in which 0.3 g of the material was dispersed in 15 mL of aqua regia and stirred for 15 min after which the sample was removed by filtration, washed with distilled water and dried under vacuum for 4 h (Fig. S1c†).

For comparison purposes, YTOS was also prepared using the SSR and flux-assisted methods in sealed quartz tubes. In the former case, Y_2O_3, Y_2S_3 and TiO_2 were combined in a stoichiometric ratio of 1 : 2 : 6 and thoroughly ground in a glovebox. Sulfur powder (HIGH PURITY CHEMICALS) was added to this

Open Access Article. Published on 13 January 2025. Downloaded on 12/31/2025 11:32:42 AM. This article is licensed under a Creative Commons Attribution 3.0 Unported Licence.

mixture at an amount equivalent to 5.0 wt% with respect to the total amount of the precursor mixture to produce a sulfur-rich environment. The materials were subsequently sealed in an evacuated quartz tube and heated to 500 °C at a rate of 10 °C min^{-1} and then heated to 800 °C at 5 °C min^{-1}. After holding at that temperature for a specific duration, followed by natural cooling, the powder was removed and then heated in air at 200 °C for 1 h to remove excess sulfur. The resulting powder was rinsed with water, recovered by filtration and dried under vacuum. The samples prepared in this manner with a duration of 96 h are herein referred to as YTOS-SSR. A specimen was also prepared using the H_2S sulfurization process in a manner similar to the SSR method, except that a 0.5 g precursor mixture was placed in an alumina boat and heated at 1150 °C for 2 h under a 50 mL min^{-1} flow of H_2S. This material is denoted as YTOS-HS. In the case of the flux-assisted method, the precursors and sulfur were thoroughly ground together with 500 wt% $CaCl_2$ in a glovebox, after which the mixture was sealed in an evacuated quartz tube. This was followed by calcination using the same heating program as employed for the SSR method. After holding at 800 °C for 3 h and allowing for natural cooling, the sample was sonicated in distilled water and recovered by filtration to remove the flux. The as-obtained powder was dried by heating under vacuum at 40 °C for 4 h. Finally, the product was heated at 200 °C in air for 1 h to remove residual sulfur and then dispersed in distilled water again by sonication. This was followed by filtration and drying under vacuum for 4 h. The resulting material is referred to as YTOS-Flux.

Material characterization

X-ray diffraction (XRD) analyses were performed using a Rigaku MiniFlex 300 system. The morphologies and compositions of the samples were assessed using field-emission scanning electron microscopy (SEM) together with energy-dispersive X-ray spectroscopy (EDS), employing a Phenom Pharos instrument (ThermoFisher Scientific) and a JEOL JSM-7800F microscope. Transmission electron microscopy (TEM) and selected area electron diffraction (SAED) analyses were carried out with a JEOL JEM-2800 and 2100F microscope. Cross-sectional samples were prepared with a focused Ga-ion beam (JEOL JIB-4600F) and an Ar-ion slicer (JEOL EM-09100IS). X-ray photoelectron spectroscopy (XPS) was performed using a PHI Quantera II instrument (ULVAC-PHI, Inc.) with a monochromatic Al Kα line source.

Photocatalytic H_2 evolution reaction

Trials involving the photocatalytic hydrogen evolution reaction were carried out in a Pyrex top-illuminated reaction vessel connected to a closed gas circulation system. Rh serving as a hydrogen evolution cocatalyst was loaded onto the sample surface by impregnation at a proportion of 1.0 wt% using $RhCl_3 \cdot 3H_2O$ as the precursor. This precursor was reduced by heating under H_2 at 300 °C for 1 h. Following this, 0.2 g of the resulting Rh/YTOS was dispersed in 150 mL of an aqueous Na_2S–Na_2SO_3 (20 mM each) solution. The YTOS-YO prepared with a 1 : 2 precursor-to-flux mass ratio was also applied to the photocatalytic O_2 evolution reaction. Prior to these trials, Co_3O_4 was deposited on the specimen as an oxygen evolution cocatalyst by an impregnation method, using $Co(NO_3)_2 \cdot 6H_2O$ as the precursor in conjunction with thermal decomposition at 300 °C for 1 h under N_2. The resulting powder was then dispersed in 150 mL of an aqueous $AgNO_3$ (20 mM) solution containing 0.2 g of La_2O_3 as the pH buffer. After completely removing air from the system by evacuation, the background pressure was adjusted to 8 kPa by introducing Ar gas. Following these steps, the suspension was irradiated with a 300 W Xe lamp equipped with a cut-off filter (L42, $\lambda > 420$ nm) while the reaction system was maintained at room temperature by circulating cooling water through the apparatus. The quantities of H_2 or O_2 evolved during the reaction were determined using an integrated gas chromatography system comprising a GC-8A gas chromatograph (Shimadzu Corp.) equipped with 5 Å molecular sieve columns and a thermal conductivity detector, using Ar as the carrier gas. The apparent quantum yield (AQY) for the photocatalytic hydrogen evolution was evaluated using the same experimental setup except for the use of a bandpass filter with a central wavelength of 420 nm. The value was calculated using the following equation:

$$\mathrm{AQY} = N_e/N_p \times 100\%$$

where N_p is the number of incident photons and N_e is the number of reacted electrons.

Results and discussion

The initial trials used the conventional SSR precursor mixture of Y_2O_3, Y_2S_3 and TiO_2 for the sulfurization procedure. This experiment produced a black powder following calcination at 800 °C for 3 h. A subsequent XRD analysis indicated that Y_2O_2S, TiS_2, Y_2S_3 and TiO_2 were present in the product mixture but YTOS was not obtained (Fig. S2†). The Y_2O_2S and TiS_2 may have formed either through the sulfurization of the original Y_2O_3 and TiO_2, respectively, or by the reaction of Y_2S_3 with TiO_2. The Y_2O_3, Y_2O_2S and TiO_2 phases all completely disappeared after sulfurization for 6 h, with only Y_2S_3 and TiS_2 remaining (Fig. 1a). To better understand the sulfurization process, either Y_2O_3 or TiO_2 was heated in a mixed CS_2/N_2 atmosphere at 800 °C. In the case of the former compound, Y_2O_2S and unreacted Y_2O_3 were detected following sulfurization for 1 h while pure Y_2S_3 was obtained after sulfurization for 3 h (Fig. 1b). These results differ from those observed using H_2S as the sulfurization reagent, which gave only Y_2O_2S (Fig. S3†). The experiment with TiO_2 yielded TiS_2 as the sole product after sulfurization (Fig. 1c). Similarly, heating a mixture of Y_2O_3 and TiO_2 under the same conditions provided Y_2S_3 and TiS_2 without other phases such as $Y_2Ti_2O_7$ or YTOS (Fig. S4†). Finally, when $Y_2Ti_2O_7$ was employed as the starting material for the sulfurization procedure, Y_2S_3 and TiS_2 were detected as the products together with unreacted $Y_2Ti_2O_7$ after sulfurization for 1 h. Upon extending the heating duration to 3 h, the $Y_2Ti_2O_7$ phase was completely decomposed and Y_2S_3 and TiS_2 were generated (Fig. 1d), indicating that CS_2 could decompose stable $Y_2Ti_2O_7$ into binary sulfides. Overall, it

 This journal is © The Royal Society of Chemistry 2025

Open Access Article. Published on 13 January 2025. Downloaded on 12/31/2025 11:32:42 AM.
This article is licensed under a Creative Commons Attribution 3.0 Unported Licence.

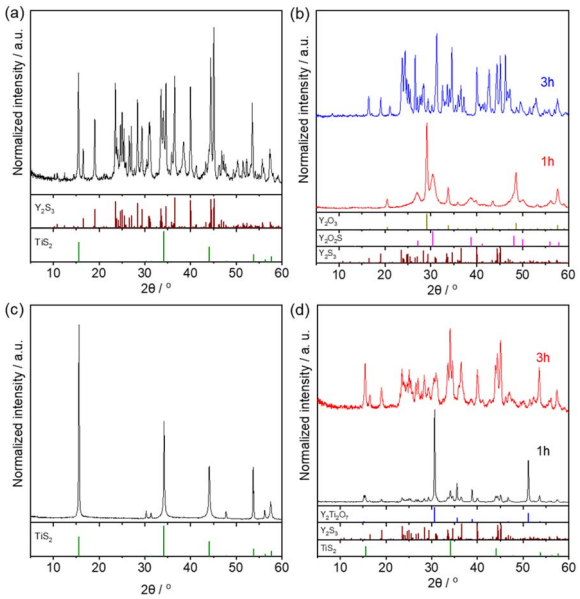

Fig. 1 XRD patterns for samples obtained by sulfurization of (a) a precursor mixture containing Y_2S_3 for 6 h, (b) Y_2O_3 for 1 or 3 h, (c) TiO_2 for 3 h, and (d) $Y_2Ti_2O_7$ for 1 or 3 h.

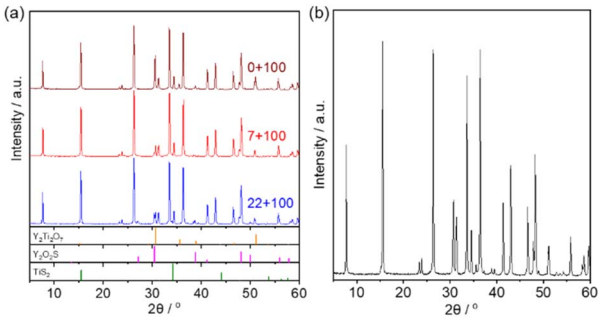

Fig. 2 XRD patterns for (a) YTOS-YOYS and (b) YTOS-YO specimens produced by flux-assisted sulfurization. The numerical values in (a) indicate the flow rates for the CS_2/N_2 mixture combined with a 100 mL min^{-1} flow of N_2.

was not possible to synthesize YTOS using these three types of precursors *via* the CS_2 sulfurization method. When the same heating program was used in conjunction with the SSR method in a sealed evacuated quartz tube, the product consisted of a mixture of YTOS and various intermediates ($Y_2Ti_2O_7$, Y_2O_2S and TiS_2) after 3 h. YTOS became the main product after extending the heating duration to 12 h or longer (Fig. S5†). It is evident that the sulfurization activity of CS_2 was too strong, resulting in the sulfurization of Y and Ti compounds before the formation of YTi complex compounds. Even if such complexes were formed, they were then excessively sulfurized and so decomposed into Y_2S_3 and TiS_2.

The use of flux reagents was expected to promote the inter-diffusion of Y and Ti components to produce YTOS as a stable phase in a relatively short time span. Accordingly, a mixture of Y_2O_3, Y_2S_3 and TiO_2 together with a $CaCl_2$ flux was employed to carry out the sulfurization procedure. In contrast to the trials without a flux, YTOS was found as the major phase together with the byproducts Y_2O_2S and TiS_2 upon setting the CS_2/N_2 flow rate to 22 mL min^{-1}. No impurities derived from the flux were detected. In addition, YTOS with a reduced concentration of impurities was found when the CS_2/N_2 flow rate was decreased to 7 mL min^{-1} (Fig. 2a). Notably, YTOS was formed even when the CS_2/N_2 flow rate was zero, meaning that the sample was calcined in a N_2 flow. However, the concentration of $Y_2Ti_2O_7$ present as an impurity was significantly increased under these conditions, due to the decomposition of YTOS at the interface between the flux and the N_2 stream. The primary role of CS_2 in the procedure detailed above was evidently to prevent the oxidation of YTOS rather than to provide sulfide ions during its formation. The successful formation of the YTOS phase in these experiments is also ascribed to the enhanced mass transfer resulting from the presence of the $CaCl_2$ flux. A similar effect was observed in the experiments using the SSR method. In order to generate YTOS by the SSR method, sulfur had to be added as a chemical vapor transport reagent within the sealed quartz tube. In the absence of sulfur, only the intermediate phases $Y_2Ti_2O_7$, Y_2O_2S and TiS_2 were formed.[37] For comparison purposes, YTOS was also synthesized using the flux-assisted method together with a sealed evacuated quartz tube (Fig. S6†).

Additional work showed that YTOS could be produced using Y_2O_3 and TiO_2 oxides as the starting materials in conjunction with the flux-assisted sulfurization process (Fig. 2b). In this case, the precursor mixture did not contain a sulfur source and so the CS_2 provided sulfur during the formation of the YTOS crystals. A previous study indicated that YTOS can be formed *via* intermediate phases $Y_2Ti_2O_7$, Y_2O_2S and TiS_2 during the SSR synthesis process. Indeed, these intermediate phases were also detected after heating a mixture of oxide precursors in the presence of a $CaCl_2$ flux under a CS_2 atmosphere. It is apparent that $Y_2Ti_2O_7$ was formed by the reaction of Y_2O_3 and TiO_2 whereas Y_2O_2S and TiS_2 could be generated by the sulfurization of Y_2O_3 and TiO_2. The flux enhanced the mass transfer rate in the reaction mixture and accelerated the synthesis of YTOS. In the absence of the flux, Y_2S_3 was evolved prior to the formation of YTOS due to the oversulfurization effect, as discussed above.

Fig. 3 presents SEM images of YTOS specimens prepared by the SSR, flux-assisted and flux-assisted sulfurization methods with two types of precursors. Compared with the results obtained using the SSR method, the particle size was reduced when the flux was included in the preparation procedure. The YTOS-flux was found to consist of plate-like sheets with a wide range of particle sizes, whereas the YTOS-YOYS crystals were even smaller than the YTOS-flux particles. Plate-like particles were also found in the sample synthesized from Y_2O_3 and TiO_2 and the average long-axis size of these particles was approximately 700 nm. These plates were therefore larger than those comprising the YTOS-YOYS (600 nm) but smaller than the YTOS-SSR (4.0 μm) and YTOS-Flux (2.0 μm) particles. Moreover, the particle size of YTOS-YSYO and YTOS-YO was more homogenous with respect to the YTOS-SSR and YTOS-flux

Open Access Article. Published on 13 January 2025. Downloaded on 12/31/2025 11:32:42 AM.
This article is licensed under a Creative Commons Attribution 3.0 Unported Licence.

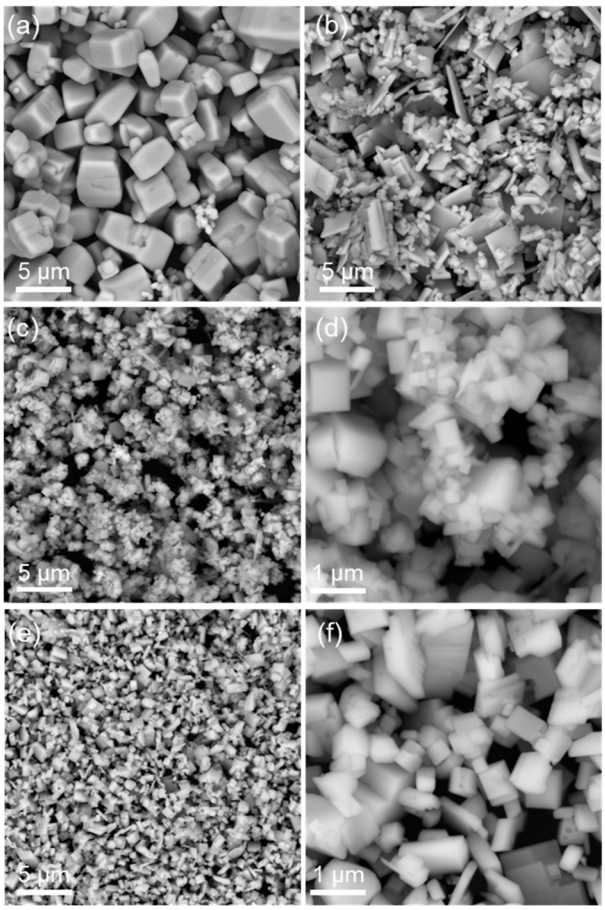

Fig. 3 SEM images of (a) YTOS-SSR, (b) YTOS-flux, (c and d) YTOS-YOYS, and (e and f) YTOS-YO samples.

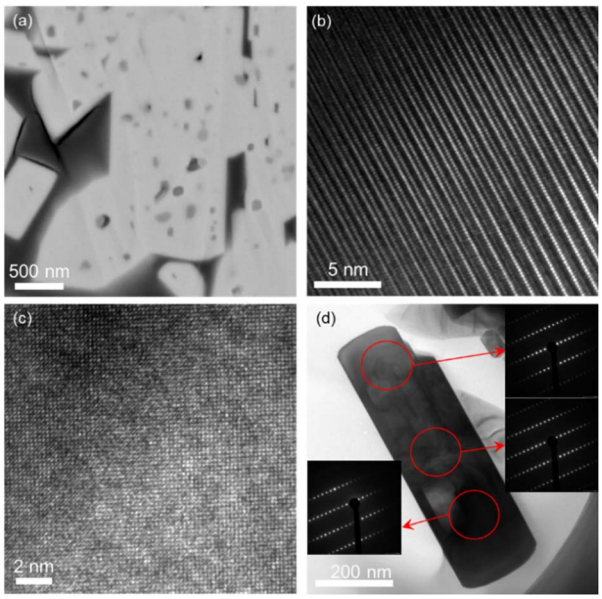

Fig. 4 (a) Cross-sectional SEM image, TEM images acquired along the (b) side and (c) basal surfaces, and (d) SAED patterns obtained from different regions of a YTOS-YO specimen.

samples (Fig. S7†). The use of oxide precursors resulted in the formation of YTOS having monodisperse particle sizes with more regular shapes compared with the materials generated using the Y_2S_3-containing precursor mixture, suggesting improved crystallinity in the former material. In addition, the elemental composition of YTOS-YO was close to the stoichiometric ratio of YTOS based on the EDS analysis (Fig. S8†). The YTOS-YO sample was further assessed by acquiring cross-sectional SEM and TEM images. Regular particles with porous structures were observed in the SEM images (Fig. 4a) while high-resolution TEM images together with SAED analyses indicated a high degree of crystallinity (Fig. 4b–d and S9a†). The formation of voids inside the YTOS particles was confirmed by the TEM images, and the morphology of these voids was found to be similar to that of the secondary particles (Fig. S9b†). It is difficult to explain the formation of such voids in the YTOS single crystals. However, it is possible that these crystals were formed *via* the alignment of smaller YTOS single crystals, such that interparticle voids were trapped. Hence, it may be possible to further decrease the particle size of the YTOS by optimizing the synthesis method to inhibit aggregation of the primary YTOS particles.

Taking into account the monodisperse particles and the exceptional crystallinity of the YTOS-YO prepared with oxide precursors, further experiments were performed to investigate the effects of preparation conditions on the characteristics of the material. The YTOS with a trace amount of carbon impurities was formed with a loading amount of 0.6 g of the mixture. The impurities disappeared and the XRD patterns were nearly the same when the loading amount was increased to 1.5 g and 3.0 g. Further increasing the loading amount to 4.5 g resulted in an increased amount of $Y_2Ti_2O_7$ impurity (Fig. S10†). The effect of the precursor-to-flux mass ratio was studied and XRD analysis indicated that nearly pure YTOS was obtained with ratios of 1 : 5, 1 : 3 or 1 : 2. However, when this ratio was decreased to 1 : 1, impurities such as Y_2O_2S and TiS_2 appeared (Fig. S11†). SEM images indicated that specimens generated using ratios of 1 : 5, 1 : 3 or 1 : 2 all had similar particle morphologies whereas characteristic intermediate phase particles were observed in YTOS prepared with a 1 : 1 ratio (Fig. S12†). In additional experiments, the CS_2 partial pressure was varied by changing the flow rate of the N_2 used for dilution purposes while maintaining the original CS_2/N_2 flow rate. Upon increasing the N_2 flow rate from 100 to 200 mL min^{-1}, the amount of $Y_2Ti_2O_7$ formed as an impurity was increased significantly. This effect can be ascribed to the decomposition of YTOS resulting from the reduced CS_2 partial pressure. Further decreasing the N_2 flow rate to 50 mL min^{-1} generated YTOS together with higher proportions of Y_2O_2S and TiS_2 due to excessive sulfurization. It is worth noting that carbon was also detected as an impurity when the N_2 flow rate was decreased to zero, indicating that carbon from decomposed CS_2 was readily deposited on the sample when the gas flow rate was too low (Fig. S13a†). Similarly, more $Y_2Ti_2O_7$ was produced upon decreasing the CS_2/N_2 flow rate at a fixed N_2 flow rate, whereas greater amounts of Y_2O_2S and TiO_2 were generated after increasing the CS_2/N_2 flow rate (Fig. S13b†). In other trials, varying the heating duration

 This journal is © The Royal Society of Chemistry 2025

Open Access Article. Published on 13 January 2025. Downloaded on 12/31/2025 11:32:42 AM.
This article is licensed under a Creative Commons Attribution 3.0 Unported Licence.

was found to result in a more intense $Y_2Ti_2O_7$ XRD peak in addition to the YTOS peak after a 15 min duration. YTOS was identified as the primary phase at a duration of 1 h and the XRD patterns remained unchanged by prolonging the reaction time to 6 h. These data suggest that the crystalline YTOS was resistant to CS_2 sulfurization once formed in the presence of the $CaCl_2$ flux (Fig. S13c†). Finally, an increased amount of $Y_2Ti_2O_7$ was synthesized upon increasing the heating rate above 500 °C from 5 to 10 °C min^{-1}, while increased amounts of Y_2O_2S and TiS_2 were detected upon decreasing the heating rate to 2.5 °C min^{-1} (Fig. S13d†). These results indicate that the product composition was highly sensitive to the preparation conditions. It will evidently be vital to optimize the synthetic parameters when scaling up the reaction to produce large amounts of oxysulfide materials. Y_2O_2S and TiS_2 were typically generated as impurities due to oversulfurization, whereas $Y_2Ti_2O_7$ resulted from insufficient sulfurization. Based on these data, it should be possible to tune the multiple synthesis parameters to obtain desired products in high purities.

The $Y_2Ti_2O_7$ prepared by heating Y_2O_3 and TiO_2 at 1000 °C for 6 h in air (Fig. S14a†) was also used as a precursor in a flux-assisted sulfurization procedure. Following sulfurization for 3 h, YTOS was found to have formed, although a large amount of unreacted $Y_2Ti_2O_7$ also remained (Fig. S14b†). Neither Y_2O_2S nor TiS_2 was identified by XRD analyses. Hence, the $Y_2Ti_2O_7$ appears to have been directly converted to YTOS using the CS_2 sulfurization method together with a flux, but the associated kinetics were slower compared with those during the *in situ* formation of $Y_2Ti_2O_7$ followed by reaction with Y_2O_2S and TiS_2. Large YTOS crystals together with unreacted $Y_2Ti_2O_7$ were observed in SEM images (Fig. S14c†). These results can be ascribed to the aggregation of $Y_2Ti_2O_7$ particles during the formation of the YTOS crystals.

To summarize, the CS_2 sulfurization process was examined with and without the use of a flux and with three different types of precursors. Among these, the combination of Y_2O_3 and TiO_2 appears to be the most suitable for the preparation of YTOS by flux-assisted sulfurization. Using these two binary oxides as starting materials, it is possible to remove any effect of variations in the Y_2S_3 purity. This process could also reduce the costs associated with the large-scale production of YTOS as a photocatalyst. In addition, pure YTOS can be generated with smaller particle sizes and a higher degree of crystallinity compared with the products obtained from the SSR and flux-assisted methods, both of which require a closed system for synthesis.

The photocatalytic H_2 evolution activities of the YTOS samples prepared using the different procedures were also investigated. Prior to these experiments, Rh was loaded onto the YTOS surfaces *via* an impregnation method. The YTOS-YOYS was found to exhibit lower H_2 evolution activity than YTOS-SSR, YTOS-flux and YTOS-HS (Fig. 5a). In contrast, the performance of YTOS-YO prepared with a precursor-to-flux mass ratio of 1 : 5 was comparable to that of YTOS-SSR but still lower than that of YTOS-Flux. Furthermore, the activity of YTOS-YO could be enhanced by increasing the reaction duration to 3 h. Further prolonging the heating time decreased the level of activity (Fig. 5b), presumably as a result of oversulfurization of the

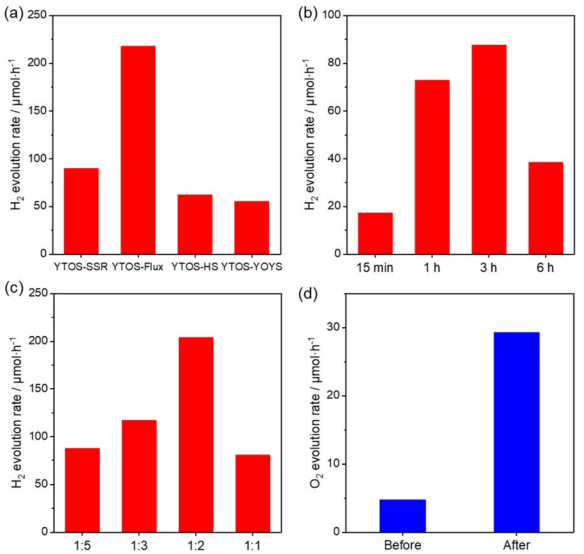

Fig. 5 Photocatalytic H_2 evolution activity of (a) samples prepared using different methods, and of YTOS-YO specimens synthesized using various (b) heating durations and (c) precursor-to-flux mass ratios. (d) Photocatalytic O_2 evolution activity of YTOS-YO before and after acid treatment.

catalyst surfaces because the crystal structure and morphology were not obviously changed. This was further confirmed by XPS analysis, where the overall peak profiles of these two samples were similar to each other, but the peak area ratio of sulfur to other elements was changed (Fig. S15†). Specifically, the peak area ratio of S $2p_{1/2}$ to Y $3d_{5/2}$ was increased from 0.11 to 0.17. Similarly, the peak area ratio of S 2s to Y $3d_{5/2}$ was increased from 0.18 to 0.22. Such results indicated that the content of sulfur element on the surface was increased due to oversulfurization. This finding is consistent with the observation of significantly decreased activity following additional sulfurization of YTOS-SSR in a CS_2 atmosphere in the presence/absence of flux (Fig. S16†). Importantly, the H_2 evolution rate for YTOS-YO was increased upon decreasing the amount of flux and reached a maximum at a ratio of 1 : 2. The H_2 evolution rate was two times higher than that for YTOS-SSR and comparable to that for the YTOS-flux (Fig. 5c), indicating the high quality of the YTOS-YO sample. An AQY of 3.5% was obtained under irradiation with 420 nm monochromatic light. Further decreasing the amount of flux reduced the activity of the photocatalyst, which can be attributed to an increased amount of impurities. Noting that the best activity of the sample prepared by the flux-assisted sulfurization method with CS_2 is much higher than that of the sample with H_2S, it is still lower compared with the state-of-the-art YTOS prepared in a sealed quartz tube (Table S1†). Therefore, there is still great room to improve the performance of the sample prepared by the flux-assisted sulfurization method. The trace amount of the $Y_2Ti_2O_7$ intermediate phase was usually found after the formation of YTOS, which can be ascribed to the weighing errors and the non-ideal purity of the precursors. Since the band gap of $Y_2Ti_2O_7$ was around 3.5 eV,[38] which cannot respond to visible light, the influence of the $Y_2Ti_2O_7$ impurity on the performance was negligible. The sample

Open Access Article. Published on 13 January 2025. Downloaded on 12/31/2025 11:32:42 AM. This article is licensed under a Creative Commons Attribution 3.0 Unported Licence.

prepared with a precursor-to-flux mass ratio of 1 : 2 was also applied to the photocatalytic O_2 evolution reaction using Co_3O_4 as the co-catalyst, but exhibited much lower activity than YTOS-SSR (Fig. S17†). According to previous reports, a post-synthesis treatment in an acidic solution can greatly affect the performance of YTOS, especially when the sample is prepared by a flux-assisted method. This effect occurs because an amorphous layer is usually formed on the surface of the material.[39] Therefore, in the present work, a YTOS specimen was immersed in aqua regia at room temperature for 15 min. Analyses of this material by XRD and SEM (Fig. S18†) showed no changes, indicating the superior stability of the crystalline YTOS in an acidic solution. The H_2 evolution rate for the specimen did not change significantly but the stability of the material was improved, which was further confirmed by the cyclic performance test (Fig. S19†). From the TEM images, the lattice fringe of the sample after acid treatment was observed more clearly than that of the sample without acid treatment, indicating that the surface amorphous layer could be removed by the acid treatment. After cocatalyst loading, Rh particles with a more regular shape and larger particle size were observed on the acid-treated sample (Fig. S20†). This indicated that Rh^{3+} was more easily adsorbed on the acid-treated sample, leading to improved contact between the cocatalyst and the surface after chemical reduction. Interestingly, the O_2 evolution rate of the sample increased six-fold after the acid treatment (Fig. 5d). In addition, a similar O_2 evolution rate (33 μmol h^{-1}) was obtained after acid treatment in the case of the sample prepared with a precursor to flux ratio of 1 : 5. These results indicated that the performance of the as-prepared sample can be further enhanced through appropriate surface modification.

Conclusions

CS_2 was utilized as a sulfurization reagent in the preparation of YTOS intended for use as a photocatalyst, and crystalline YTOS was generated in the presence of a flux. In contrast, in the absence of a flux, Y_2S_3 and TiS_2 were formed as the final products due to oversulfurization. This outcome is attributed to the strong sulfurization activity of CS_2 and the insufficient mass transfer between the starting materials. The products were also sensitive to the synthesis conditions, and YTOS prepared from Y_2O_3 and TiO_2 precursors showed an especially high degree of crystallinity and reduced particle sizes compared with the samples prepared by the SSR and flux-assisted methods. The as-obtained sample with a precursor-to-flux ratio of 1 : 2 exhibited photocatalytic H_2 evolution activity superior to that of the YTOS specimen synthesized by the SSR method and sulfurization method with H_2S, and comparable to that of the YTOS sample prepared using the flux-assisted method. This sample also showed photocatalytic O_2 evolution activity after being loaded with Co_3O_4 as a cocatalyst. This activity could be enhanced by carrying out an acid treatment prior to deposition of the cocatalyst. These results suggest that flux-assisted sulfurization with CS_2 is a promising approach for the large-scale preparation of oxysulfide photocatalysts for solar hydrogen production.

Data availability

The data supporting this article have been included as part of the ESI.† Data are also available upon request from the authors.

Author contributions

K. K., T. H., T. T. and K. D. supervised the research. L. L., Q. L., Y. K., and C. G. carried out the experiments. M. N. and D. L. performed the cross-sectional SEM and TEM analysis. The manuscript was written through contributions of all authors. All authors have given approval to the final version of the manuscript.

Conflicts of interest

The authors declare no competing financial interests.

Acknowledgements

This research was supported by the Artificial Photosynthesis Project (ARPChem) of the New Energy and Industrial Technology Development Organization (NEDO). A part of this work was supported by the "Advanced Research Infrastructure for Materials and Nanotechnology in Japan (ARIM)" of the Ministry of Education, Culture, Sports, Science and Technology (MEXT), Grant Number JPMXP1223UT0004.

References

1 X. Tao, Y. Zhao, S. Wang, C. Li and R. Li, *Chem. Soc. Rev.*, 2022, **51**, 3561–3608.
2 Q. Wang and K. Domen, *Chem. Rev.*, 2020, **120**, 919–985.
3 L. Lin, T. Hisatomi, S. Chen, T. Takata and K. Domen, *Trends Chem.*, 2020, **2**, 813–824.
4 C. Boyer-Candalen, J. Derouet, P. Porcher, Y. Moëlo and A. Meerschaut, *J. Solid State Chem.*, 2002, **165**, 228–237.
5 Q. Wang, M. Nakabayashi, T. Hisatomi, S. Sun, S. Akiyama, Z. Wang, Z. Pan, X. Xiao, T. Watanabe, T. Yamada, N. Shibata, T. Takata and K. Domen, *Nat. Mater.*, 2019, **18**, 827–832.
6 V. Nandal, R. Shoji, H. Matsuzaki, A. Furube, L. Lin, T. Hisatomi, M. Kaneko, K. Yamashita, K. Domen and K. Seki, *Nat. Commun.*, 2021, **12**, 7055.
7 R. Li, Z. Zha, Y. Zhang, M. Yang, L. Lin, Q. Wang, T. Hisatomi, M. Nakabayashi, N. Shibata, K. Domen and Y. Li, *J. Mater. Chem. A*, 2022, **10**, 24247–24257.
8 H. Yoshida, Z. Pan, R. Shoji, V. Nandal, H. Matsuzaki, K. Seki, T. Hisatomi and K. Domen, *J. Mater. Chem. A*, 2022, **10**, 24552–24560.
9 L. Lin, V. Polliotto, J. J. M. Vequizo, X. Tao, X. Liang, Y. Ma, T. Hisatomi, T. Takata and K. Domen, *ChemPhotoChem*, 2022, **6**, e202200209.
10 S. G. Denis and S. J. Clarke, *Chem. Commun.*, 2001, 2356–2357.
11 O. J. Rutt, T. L. Hill, Z. A. Gál, M. A. Hayward and S. J. Clarke, *Inorg. Chem.*, 2003, **42**, 7906–7911.

 This journal is © The Royal Society of Chemistry 2025

Open Access Article. Published on 13 January 2025. Downloaded on 12/31/2025 11:32:42 AM. This article is licensed under a Creative Commons Attribution 3.0 Unported Licence.

12 C. Boyer, C. Deudon and A. Meerschaut, *Comptes Rendus Acad. Sci. - Ser. IIC Chem.*, 1999, **2**, 93–99.
13 M. Goga, R. Seshadri, V. Ksenofontov, P. Gütlich and W. Tremel, *Chem. Commun.*, 1999, 979–980.
14 S. V. Volkov, *Chem. Soc. Rev.*, 1990, **19**, 21–28.
15 M. J. Bojdys, J.-O. Müller, M. Antonietti and A. Thomas, *Chem.–Eur. J.*, 2008, **14**, 8177–8182.
16 A. Savateev, I. Ghosh, B. König and M. Antonietti, *Angew. Chem., Int. Ed.*, 2018, **57**, 15936–15947.
17 S. K. Gupta and Y. Mao, *J. Phys. Chem. C*, 2021, **125**, 6508–6533.
18 A. Ishikawa, T. Takata, J. N. Kondo, M. Hara, H. Kobayashi and K. Domen, *J. Am. Chem. Soc.*, 2002, **124**, 13547–13553.
19 G. Ma, S. Chen, Y. Kuang, S. Akiyama, T. Hisatomi, M. Nakabayashi, N. Shibata, M. Katayama, T. Minegishi and K. Domen, *J. Phys. Chem. Lett.*, 2016, **7**, 3892–3896.
20 G. Ma, Y. Kuang, D. H. K. Murthy, T. Hisatomi, J. Seo, S. Chen, H. Matsuzaki, Y. Suzuki, M. Katayama, T. Minegishi, K. Seki, A. Furube and K. Domen, *J. Phys. Chem. C*, 2018, **122**, 13492–13499.
21 L. Lin, P. Kaewdee, V. Nandal, R. Shoji, H. Matsuzaki, K. Seki, M. Nakabayashi, N. Shibata, X. Tao, X. Liang, Y. Ma, T. Hisatomi, T. Takata and K. Domen, *Angew. Chem., Int. Ed.*, 2023, **62**, e202310607.
22 M. Nakabayashi, K. Nishiguchi, X. Liang, T. Hisatomi, T. Takata, T. Tsuchimochi, N. Shibata, K. Domen and S. L. Ten-no, *J. Phys. Chem. C*, 2023, **127**, 7887–7893.
23 X. Liang, J. J. M. Vequizo, L. Lin, X. Tao, Q. Zhu, M. Nakabayashi, D. Lu, H. Yoshida, A. Yamakata, T. Hisatomi, T. Takata and K. Domen, *Adv. Sci.*, 2024, 2412326.
24 H. Kato, K. Asakura and A. Kudo, *J. Am. Chem. Soc.*, 2003, **125**, 3082–3089.
25 K. Maeda, *ACS Catal.*, 2013, **3**, 1486–1503.
26 P. Zhang, J. Zhang and J. Gong, *Chem. Soc. Rev.*, 2014, **43**, 4395–4422.
27 A. Kudo, K. Omori and H. Kato, *J. Am. Chem. Soc.*, 1999, **121**, 11459–11467.
28 D. Jing and L. Guo, *J. Phys. Chem. B*, 2006, **110**, 11139–11145.
29 Y. Zhang, X. Wu, Z.-H. Wang, Y. Peng, Y. Liu, S. Yang, C. Sun, X. Xu, X. Zhang, J. Kang, S.-H. Wei, P. F. Liu, S. Dai and H. G. Yang, *J. Am. Chem. Soc.*, 2024, **146**, 6618–6627.
30 L. Lin, Z. Lin, J. Zhang, X. Cai, W. Lin, Z. Yu and X. Wang, *Nat. Catal.*, 2020, **3**, 649–655.
31 A. Ishikawa, Y. Yamada, T. Takata, J. N. Kondo, M. Hara, H. Kobayashi and K. Domen, *Chem. Mater.*, 2003, **15**, 4442–4446.
32 A. Ishikawa, T. Takata, T. Matsumura, J. N. Kondo, M. Hara, H. Kobayashi and K. Domen, *J. Phys. Chem. B*, 2004, **108**, 2637–2642.
33 Z. Pan, H. Yoshida, L. Lin, Q. Xiao, M. Nakabayashi, N. Shibata, T. Takata, T. Hisatomi and K. Domen, *Res. Chem. Intermed.*, 2021, **47**, 225–234.
34 C. W. Dunnill, Z. A. Aiken, A. Kafizas, J. Pratten, M. Wilson, D. J. Morgan and I. P. Parkin, *J. Mater. Chem.*, 2009, **19**, 8747–8754.
35 N. Sato and A. Kirishima, *J. Nucl. Mater.*, 2011, **414**, 324–327.
36 M. Nasilowski, B. Mahler, E. Lhuillier, S. Ithurria and B. Dubertret, *Chem. Rev.*, 2016, **116**, 10934–10982.
37 L. Lin, M. Nakabayashi, D. Lu, T. Hisatomi, T. Takata and K. Domen, *Chem. Mater.*, 2024, **36**, 1612–1620.
38 R. Abe, M. Higashi, K. Sayama, Y. Abe and H. Sugihara, *J. Phys. Chem. B*, 2006, **110**, 2219–2226.
39 H. Yoshida, Z. Pan, R. Shoji, V. Nandal, H. Matsuzaki, K. Seki, L. Lin, M. Kaneko, T. Fukui, K. Yamashita, T. Takata, T. Hisatomi and K. Domen, *Angew. Chem., Int. Ed.*, 2023, **62**, e202312938.